Early White Matter Microstructure Alterations in Infants with Down Syndrome

Omar Azrak, MD[1]; Dea Garic, PhD[1,2]; Aleeshah Nasir, BA[1]; Meghan R. Swanson, PhD[3]; Rebecca L. Grzadzinski, PhD[1,2]; Khalid Al-Ali, MD[4]; Mark D. Shen, PhD[1,2]; Jessica B. Girault, PhD[1,2]; Tanya St. John, PhD[5]; Juhi Pandey, PhD[6]; Lonnie Zwaigenbaum, MD[7]; Annette M. Estes, PhD[5]; Jason J. Wolff, PhD[3]; Stephen R. Dager, MD[8]; Robert T. Schultz, PhD[6]; Alan C. Evans, PhD[9]; Jed T. Elison, PhD[10]; Essa Yacoub, PhD[11]; Sun Hyung Kim, PhD[1]; Robert C. McKinstry, MD, PhD[12]; Guido Gerig, PhD[13]; John R. Pruett Jr., MD, PhD[14]; Joseph Piven, MD[1,2]; Kelly N. Botteron, MD[14]; Heather Hazlett, PhD[1,2*]; Natasha Marrus, MD, PhD[14*]; Martin A. Styner, PhD[1*]; for the Infant Brain Imaging Study (IBIS) Network

**shared senior authorship*

Author affiliations:

1. Department of Psychiatry, University of North Carolina at Chapel Hill School of Medicine, Chapel Hill, NC, USA
2. Carolina Institute for Developmental Disabilities, University of North Carolina at Chapel Hill School of Medicine, Chapel Hill, NC, USA
3. Department of Pediatrics, University of Minnesota, Minneapolis, MN, USA
4. Department of Psychiatry, Indiana University School of Medicine, Indianapolis, IN, USA
5. University of Washington Autism Center, University of Washington, Seattle, WA, USA
6. Center for Autism Research, Children's Hospital of Philadelphia, University of Pennsylvania Perelman School of Medicine, Philadelphia, PA, USA
7. Autism Research Centre, Department of Pediatrics, University of Alberta, Edmonton, Canada
8. Center on Human Development and Disability, University of Washington, Seattle, WA, USA
9. McConnell Brain Imaging Centre, Montreal Neurological Institute, McGill University, Montréal, Quebec, Canada
10. Institute of Child Development, University of Minnesota, Minneapolis, MN, USA
11. Department of Radiology, University of Minnesota, Minneapolis, MN, USA
12. Mallinckrodt Institute of Radiology, Washington University School of Medicine, St. Louis, MO, US
13. Tandon School of Engineering, New York University, New York, NY, USA
14. Department of Psychiatry, Washington University School of Medicine, St. Louis, MO, USA

Corresponding author:

Omar Azrak, MD
Department of Psychiatry, School of Medicine
The University of North Carolina at Chapel Hill
334 Emergency Room Dr
Chapel Hill, NC 27599
T: (919) 884-8733
Omar_azrak@med.unc.edu

Abstract

Importance: Down syndrome, resulting from trisomy 21, is the most prevalent chromosomal disorder and a leading cause of intellectual disability. Despite its significant impact on brain development, research on the white matter microstructure in infants with Down syndrome remains limited.

Objective: To investigate early white matter microstructure in infants with Down syndrome using diffusion tensor imaging (DTI) and neurite orientation dispersion and density imaging (NODDI).

Design: Infants were recruited and scanned between March 2019 and May 2024 as participants in prospective studies conducted by the Infant Brain Imaging Study (IBIS) Network. Data were analyzed in October 2024.

Setting: Data collection occurred at five research centers in Minnesota, Missouri, North Carolina, Pennsylvania, and Washington.

Participants: Down syndrome and control infants were scanned at 6 months of age. Control infants had no Down syndrome diagnosis and either had a typically developing older sibling or, if they had an older sibling with autism, were confirmed not to meet clinical best estimate criteria for an autism diagnosis.

Exposure: Diagnosis of Down syndrome.

Main Outcomes and Measures: The outcome of interest was white matter microstructure quantified using DTI and NODDI measures.

Results: A total of 49 Down syndrome (28 [57.14%] female) and 37 control (18 [48.65%] female) infants were included. Infants with Down syndrome showed significant reductions in fractional anisotropy and neurite density index across multiple association tracts, particularly in the inferior fronto-occipital fasciculus and superior longitudinal fasciculus II, consistent with reduced structural integrity and neurite density. These tracts also demonstrated increased radial diffusivity, suggesting delayed myelination. The inferior fronto-occipital fasciculus and uncinate fasciculus exhibited increased neurite dispersion and fanning in Down syndrome infants, reflected by elevated orientation dispersion index. Notably, the optic tracts in Down syndrome infants exhibited a distinct pattern of elevated fractional anisotropy and axial diffusivity, and lower radial diffusivity and orientation dispersion index, suggesting an early maturation of these pathways.

Conclusions and Relevance: This first characterization of white matter microstructure in Down syndrome infants reveals widespread white matter developmental delays. These findings provide new insights into the early neurodevelopment of Down syndrome and may inform early therapeutic interventions.

Introduction

Down syndrome (DS), caused by trisomy 21, is the most common genetic cause of intellectual disability, affecting approximately 1 in 600 newborns.[1,2] It is a lifelong neurodevelopmental disorder characterized by heterogeneous presentation, susceptibility to regression in childhood, and increased incidence of Alzheimer's disease (AlzD) in adulthood.[3-5] Neuroimaging research in DS has primarily focused on older children and adults, consistently revealing volumetric brain reductions and white matter (WM) integrity alterations that contribute to cognitive and functional challenges.[6-9] While previous studies in infants with DS have examined brain volume,[10-12] no research has investigated WM microstructure at this early stage.

Infancy is a critical period of brain development, particularly in WM maturation, marked by rapid myelination, heightened plasticity, and the establishment of neural pathways.[13,14] Understanding neurodevelopmental differences at infancy can (a) provide insight into how atypical neurodevelopmental trajectories emerge, (b) establish a foundation for longitudinal studies to determine how these trajectories evolve and whether they predict later behavioral and functional outcomes, and (c) identify optimal windows for mechanistically-informed interventions aimed at improving long-term cognitive and adaptive functioning in DS.[15,16]

Diffusion MRI, predominantly diffusion tensor imaging (DTI), has been instrumental in identifying WM abnormalities such as changes in fiber integrity and microstructural disruptions associated with demyelination and axonal damage.[17-19] DTI assumes a single dominant fiber orientation per voxel, making it difficult to interpret in regions with intersecting fibers.[20] To address this challenge, we employ Neurite Orientation Dispersion and Density Imaging (NODDI) to obtain a more nuanced view of WM microstructure.

In children and young adults, WM abnormalities have been identified in key tracts, including the inferior fronto-occipital fasciculus (IFOF), inferior longitudinal fasciculus (ILF), superior longitudinal fasciculus (SLF), corticospinal tract (CST), and uncinate fasciculus (UNC).[21-23] Thus, we hypothesize that infants with DS would exhibit lower fractional anisotropy (FA) and altered diffusivity in these tracts, reflecting delayed or atypical maturation of neural pathways critical for cognitive and motor function.

By utilizing advanced neuroimaging methods and ensuring a comprehensive assessment, the study aims to make a first attempt to characterize WM microstructure in infants with DS, marking a crucial step in understanding the neurodevelopmental trajectory of DS from its earliest stages.

Methods

Study design:

This cross-sectional study was reported following STROBE reporting guidelines. Ethical approval was obtained from institutional review boards at all sites that relied on a parent IRB at Washington University in St. Louis, and written informed consent was obtained from each participant's parent.

Participants:

DS infants were reported by parents to have a diagnosis of trisomy 21 (i.e., not partial or mosaic trisomy 21) and recruited as part of the IBIS-DS study. Control infants without DS, recruited as part of two IBIS infant studies (IBIS-DS and IBIS-Early Prediction), met one of two criteria. Either they had a TD older sibling and no sibling history of autism or neurodevelopmental disorders. Otherwise, if they had an older sibling with an autism diagnosis, they were themselves confirmed not to meet clinical best estimate criteria for an autism diagnosis at 24 months of age, based on DSM-IV-TR and DSM-5-TR. A background on the IBIS infant studies and detailed exclusion criteria are available in **eMethods in Supplement 1**.

MRI Acquisition and preprocessing:

MRI scans were acquired during natural sleep on identical Siemens Prisma 3T scanners with a 32-channel head coil. Diffusion-weighted images (DWIs) were acquired in anterior-posterior (AP) and posterior-anterior (PA) phase-encoding directions, with 102 DWI volumes acquired for each AP and PA: 8 b=0, 20 b= 400, 37 b=1500, 37 b=3000, TR= 3222ms, TE=89.20ms, 1.5mm^3 voxel, TA=12min19s. Tensors metrics were computed using only b=400 and 1500 shells, while NODDI metrics utilized all available shells. MRI processing and quality control steps are described in **eMethods in Supplement 1**.

A susceptibility artifact in the AP phase affecting the temporal poles was found in 50 scans **(eFigure 1)**. Steps taken to remove the artifact from the analyses are detailed in **eMethods in Supplement 1**.

WM Tract Measurements:

Metrics of WM microstructure were extracted via an extended UNC-NAMIC automated fiber analysis framework (the detailed process is available in **eMethods in Supplement 1**).[24,25] Drawing on previous findings in older children[21,23], we examined 6 intrahemispheric tracts bilaterally—corticofugal prefrontal, CST, IFOF, ILF, SLF II, and UNC—and 3 interhemispheric tracts: the parietal portion, splenium, and tapetum of the corpus callosum (CC). All primary analysis tracts are displayed in **Figure 1.**

Table 1 outlines DTI and NODDI parameters and their interpretations.

Statistical Analyses:

All statistical analyses were performed using general linear models (GLMs) in JMP 17 Pro.

Primary Analyses:

For each tract, a multivariate analysis of variance (MANOVA) was conducted comparing the average values of FA, RD, AD, NDI, and ODI between the DS and control groups. MD was excluded to avoid multicollinearity with AD and RD in MANOVA, while FWF was excluded due to its sensitivity to partial volume effects, particularly in tracts close to the cerebrospinal fluid (CSF), like the CC.

For tracts showing significant group differences in MANOVA, follow-up univariate analyses of variance (ANOVA) were conducted to identify the specific diffusion parameters significantly different between the two groups. All analyses were covaried by age-at-assessment in days, sex, and scan-motion quantification (defined as the number of diffusion volumes with significant artifacts or head motion greater than 2mm). To correct for multiple comparisons, Bonferroni correction was applied across all tests, accounting for 15 comparisons in MANOVA (*corrected $p<0.003$*) and 5 diffusion parameter comparisons in ANOVA (*corrected $p<0.01$*). All reported *p-values* from ANOVA tests in the Results section are corrected.

Secondary Analyses:

For tracts identified as significant in ANOVA, along-tract analyses were conducted using the Functional Analysis of Diffusion Tensor Tract Statistics (FADTTS) toolbox[45] and its corresponding graphical user interface, FADTTSter.[46] Along-tract analyses were performed for each diffusion parameter (FA, RD, AD, NDI, ODI) identified as significant in prior ANOVA tests, providing a finer-grained understanding of where differences occurred in the tract. Results were assessed visually and statistically to interpret region-specific differences in diffusion properties.

Finally, exploratory full-brain analyses were performed to examine all diffusion parameters (FA, AD, RD, MD, NDI, ODI, and FWF) across all 51 tracts (listed in **eTable 1**), and were conducted without correcting for multiple comparisons, providing a broader view of potential differences between groups.

Results

Demographics:

A total of 49 DS and 37 control infants were included. No significant differences were observed in sex (X^2=0.61,

p=0.43), age-at-assessment in days (*p*=0.12), and scan motion quantification (*p*=0.6). Gestational age was slightly higher in DS group (267 ± 9.5 days) than in control group (272 ± 9 days; *p*=0.015). Maternal age at birth was also significantly higher in DS group (36.84 ± 4.54 years) than in control group (34.16 ± 3.02 years; *p*=0.004), consistent with the increased incidence of DS with maternal age. A full summary of the demographics can be found in **Table 2**.

Analysis of Variance of Diffusion Parameter Averages:

Significant group differences were found between DS and control groups on MANOVA in the tapetum and parietal portions of the CC, as well as bilateral CST, IFOF, ILF, SLF II, and UNC. Left SLF II (*F*=12.16, *p*<.0001), right SLF II (*F*=10.73, *p*<.0001), left IFOF (*F*=10.57, *p*<.0001) and parietal CC (*F*=8.51, *p*<.0001) showed the strongest statistical differences on MANOVA. The splenium of the CC and bilateral corticofugal prefrontal tracts showed no group differences. **eTable 2** details the MANOVA results.

On ANOVA, several association tracts in DS infants showed patterns consistent with reduced structural integrity and neurite density, as evidenced by reduced FA and NDI, and delayed maturation indicated by increased RD. IFOF showed bilateral reductions in FA (Left: *β*=0.012, Cohen's-*d*=-1.37, *p*<.0001; Right: *β*=0.0087, Cohen's-*d*=-0.95, *p*<.0001), and NDI (Left: *β*=0.0069, Cohen's-*d*=-0.69, *p*<.0001; Right: *β*=0.0077, Cohen's-*d*=-0.69, *p*<.0001), and increase in RD (Left: *β*=-0.000014, Cohen's-*d*=0.94, *p*<.0001; Right: *β*=-0.000013, Cohen's-*d*=0.79, *p*<.0001) in DS group. SLF II showed bilateral reductions in FA (Left: *β*=0.012, Cohen's-*d*=-1.23, *p*<.0001; Right: *β*=0.0082, Cohen's-*d*=-0.811, *p*=0.004), and NDI (Left: *β*=0.0093, Cohen's-*d*=-0.85, *p*<.0001; Right: *β*=0.0088, Cohen's-*d*=-0.8, *p*<.0001), and increase in RD bilaterally (Left: *β*=-0.000018, Cohen's-*d*=1.04, *p*<.0001; Right: *β*=-0.000012, Cohen's-*d*=0.66, *p*<.0001) in DS group.

IFOF and UNC also showed increased neurite dispersion and fanning bilaterally reflected by elevated ODI in DS group (Left IFOF: *β*=-0.0058, Cohen's-*d*=1.21, *p*<.0001; Right IFOF: *β*=-0.0039, Cohen's-*d*=0.79, *p*=0.004; Left UNC: *β*=-0.0038, Cohen's-*d*=0.74, *p*=0.023; Right UNC: *β*=-0.005, Cohen's-*d*=0.94, *p*=0.001).

The parietal portion of the CC and bilateral CST demonstrated patterns of increased axonal integrity as indicated by elevated AD (Parietal CC: *β*=-0.000013, Cohen's-*d*=0.63, *p*=0.009; Left CST: *β*=−0.000019, Cohen's-*d*=0.84, *p*<.0001; Right CST: *β*=−0.000014, Cohen's-*d*=0.54, *p*=0.035). The tapetum of the CC showed no significant differences after correcting for multiple comparisons.

Figure 2 presents violin and box plots of the significant diffusion metrics in the bilateral CST and IFOF. **Table 3** details the ANOVA results for tracts found significant on MANOVA.

Along-Tract Analyses:

We conducted follow-up along-tract analyses for the diffusion parameters found significant in ANOVA to identify spatially-specific differences along the trajectories of fiber tracts.

Along-tract analysis of the bilateral CST revealed significant group differences in RD in the region between the midbrain and the internal capsule. The left ILF showed significant differences in RD in the ventral portion of the tract within the temporal lobe, while the left SLF II demonstrated differences in NDI and RD in the ventral portion of the tract as it extends into the frontal lobe. The right IFOF revealed consistent differences in FA, RD, and NDI across the frontal, temporal and parietal portions of the tract. Lastly, the right UNC exhibited differences in FA and ODI in the frontal portion of the tract. **eFigure 2** visualizes the significant *p*-values along the tracts.

Exploratory Analyses:

Exploratory analyses revealed distinct patterns in diffusion parameters between DS and control infants. FA values were lower in DS infants across all significant tracts except for the bilateral optic tracts, which exhibited higher FA values. MD values were consistently higher in DS infants, while both AD and RD values were higher in DS infants, with the exception of the left cingulate gyrus of the cingulum (CGC) for AD and the right optic tract for RD.

NDI values were consistently lower in DS infants across all significant tracts. ODI values varied across tracts, with some showing increases and others decreases in DS infants. FWF values were lower in DS infants in all significant tracts except for the CST bilaterally and the right hippocampal part of the cingulum (HCG).

Notably, the bilateral optic tracts were the only tracts to demonstrate higher FA and AD values, alongside lower RD and ODI values, suggesting preserved or distinct WM microstructure.

Full statistical results across all tracts are presented in **eTable 3**.

Discussion

This is the first study to examine the WM microstructure in infants with DS. Findings reveal consistent patterns of delayed WM maturation, characterized by regional differences in neurite density, axonal growth, and myelination. DS infants exhibited reduced microstructural coherence and delayed myelination across multiple intrahemispheric tracts, including the bilateral IFOF, SLF, and UNC, indicated by significantly lower FA and elevated RD compared to their control counterparts. Additionally, DS infants exhibited significantly elevated RD in motor pathways such as the bilateral CST. These findings align with prior DS research in early childhood to adulthood.[6,21-23]

Exploratory analyses showed increased MD in specific tracts, including the frontoparietal portion of the left arcuate fasciculus, left SLF II, and left corticothalamic motor and premotor pathways. In typical development, myelination progresses posterior-to-anterior and caudal-to-rostral, with occipital/parietal lobes myelination occurring between 4–6 months and frontal/temporal lobes between 6–8 months.[47-50] As such, it is expected that tracts located in the frontal regions would show relatively high MD during this developmental stage. The observation that DS infants exhibited higher MD in these tracts, compared to controls of the same age, suggests that the typical timeline of myelination is delayed or disrupted in DS infants, reflecting slower and less complete myelination.

Significant elevation in AD in DS infants was observed in both inter- and intrahemispheric tracts, including the CST, ILF, the parietal and tapetum portions of the CC, indicating alterations in axonal development during early growth. Romano et al.[22] reported elevated AD in the CST of young adults with DS, as well as forceps major and minor. In contrast, the lower AD and FA and higher RD in the left CGC and right UNC indicate regional delays in axonal development and myelination, highlighting differential vulnerability of pathways associated with attention, memory and emotional regulation.[6,51-53]

NDI was significantly reduced in DS infants across most major WM tracts, including the SLF II, IFOF, ILF, and the majority of the CC except the tapetum. Previous studies indicate that NDI typically reflects neurite density, which generally increases during the first two decades of life.[40,54] Lower NDI in DS infants suggests a slower rate of neurite packing, particularly in axons and dendrites, during this critical developmental window. Consistent with Timmers et al.[55] findings, NDI demonstrated greater sensitivity, identifying more tracts with lower values compared to FA. Combined with reductions in FA, the lower NDI provides converging evidence of global delays in WM maturation in DS infants.

Changes in ODI further emphasize regional variability in neurite structure. In DS infants, increased ODI in the bilateral IFOF, UNC, and SLF II suggests greater neurite dispersion, aligning with findings by Garic et al.[21] in school-aged children. This may reflect compensatory reorganization, such as axonal sprouting or delayed pruning, in response to reduced neurite density, as indicated by lower NDI.[56,57]

In our exploratory analyses, significant reductions in FWF were observed in the CC (body, motor, parietal) and corticothalamic motor and right premotor tracts, which also showed concurrent reductions in NDI. This pattern suggests reduced neurite density without evidence of neuroinflammation. While direct evidence for elevated FWF in older individuals with DS is insufficient, increased FWF has been documented in older adults with AlzD.[58,59] DS is

associated with early onset and increased prevalence of AlzD, purportedly due to the triplicated amyloid precursor protein on chromosome 21.[5,60,61] Thus, increased FWF in older DS individuals may reflect neurodegeneration or inflammation similar to that seen in AlzD. However, the reduced FWF observed in DS infants suggests an absence of inflammatory or degenerative processes at this stage, highlighting the need for longitudinal studies to distinguish the pathological changes in WM across the lifespan.

The optic tracts exhibit a distinct developmental profile, suggesting an early maturation of sensory pathways relative to higher-order systems. Infants with DS exhibited higher FA in the optic tracts bilaterally, consistent with findings from Gunbey et al.[23], who observed elevated FA in the right optic tract of two-year-old children with DS. This increase in FA, alongside elevated AD, suggests a more linear and organized axonal structure, indicative of preserved neurite density in this sensory pathway. Furthermore, reduced ODI in the optic tracts aligns with these findings, reflecting less dispersion and greater coherence in fiber orientation, consistent with early maturation typical of the visual pathway.[62,63] However, this early structural advantage does not necessarily translate to functional gains over time, as studies show that visual acuity plateaus after two years in children with DS,[64] while it continues to improve in TD peers.[65,66]

Along-tract analyses offer a detailed spatially specific assessment of WM changes compared to whole-tract average diffusion parameters.[67,68] Findings revealed localized alterations in the bilateral CST, left SLF II and ILF, and right IFOF and UNC. However, the absence of significant along-tract findings in other tracts, despite group differences detected in average parameter analyses, could be attributed to the increased number of comparisons required by along-tract approaches, which demand a larger sample size to detect significant localized changes along the tracts. Our findings demonstrate that WM microstructural alterations emerge early in DS infants, mirroring patterns observed in later developmental stages,[6-8,21-23,60] underscoring the importance of exploring this underrepresented field in DS neurodevelopment. Early interventions and therapies have been shown to improve outcomes in individuals with DS,[69] and WM may serve as a valuable biomarker for monitoring these interventions, as it has shown to change in response to treatment in children and adults.[70] Notably, a prior clinical trial reported improvements in WM connectivity following treatment in children with autism.[71] This study represents a crucial foundation for understanding the neurobiology of DS and identifying early WM alterations that may inform optimal windows for mechanistically-derived interventions aimed at improving long-term outcomes.

A key strength of our study is its larger sample of DS and control infants compared to previous studies in toddlers, the largest of which[23] included only 10 DS and 8 control individuals. The larger sample size enhances the reliability and generalizability of our findings. The use of multishell diffusion imaging allowed us to obtain and examine both DTI and NODDI data in DS infants. NODDI distinguishes intra-neurite, extra-neurite, and CSF compartments, estimating neurite density and orientation dispersion.[40,72,73] These measures complement traditional DTI, helping disentangle the effects of axonal density, myelination, and neurite organization.[74,75]

Limitations and future directions:

This study has a few limitations. A larger sample size would improve the ability to detect smaller effects in along-tract analyses. Additionally, the observed susceptibility artifact, as described in the **eMethods in Supplement 1**, necessitated a more stringent definition of certain tracts, which could have influenced the findings in the affected tracts. Future research should include longitudinal follow-up to chart WM microstructure development in DS from infancy to childhood, as well as examining how WM microstructure in infancy correlates with behavioral, language, and cognitive outcomes during childhood, potentially providing a predictive tool for these developmental outcomes.

Conclusion

Our findings reveal distinct patterns of delayed WM maturation in DS infants, marked by reduced myelination, lower neurite density, and increased neural dispersion in fibers critical for higher-order cognitive and motor functions, providing an early window into the microstructural abnormalities that may underlie later cognitive and motor delays.

By employing advanced diffusion imaging techniques, this study examines WM microstructure in DS infants, addressing a significant gap in research that has largely focused on older children and adults.

These findings lay a foundation for future longitudinal studies to explore how early WM alterations relate to cognitive, behavioral, and motor outcomes in DS, and will be essential for identifying critical windows for targeted clinical interventions aimed at supporting WM maturation and mitigating developmental delays.

Acknowledgements

Information on author access to data: Dr. Azrak had full access to all of the data in the study and takes responsibility for the integrity of the data and the accuracy of the data analysis.

Disclosure of potential conflicts of interest: Dr. Robert McKinstry holds stock options in Turing Medical and serves as a paid member of its medical advisory board. He also receives travel, lodging, and meal support from Siemens Healthcare and Radiaction, as well as meal support from Hyperfine.

Funding/Support: This study was supported by grants from the National Institutes of Health (R01HD088125, K01HD109445, K23HD112809, R01HD055741, R01MH118362, R01MH118362–02S1, P50HD103573-8084, T32HD040127, K01MH122779).

Role of the Funder/Sponsor: The funder had no role in the design and conduct of the study; collection, management, analysis, and interpretation of the data; preparation, review, or approval of the manuscript; and decision to submit the manuscript for publication.

Previous presentations: Preliminary results were presented at the Flux 2024 Congress in Baltimore, MD on September 29, 2024. The work is not being considered for any future meetings.

Use of artificial intelligence: The authors used ChatGPT (version 4o, accessed via ChatGPT Plus) by OpenAI for writing assistance in the development of the manuscript. This tool was used between November 2024 and February 2025 to refine wording, enhance clarity, and improve the readability of various sections. At no point did the AI generate original scientific content, conduct data analysis, or make independent claims about the study findings. The authors take full responsibility for the accuracy, integrity, and originality of the manuscript and its content.

References

1. Stallings EB, Isenburg JL, Rutkowski RE, et al. National population-based estimates for major birth defects, 2016-2020. *Birth Defects Res*. 2024;116(1):e2301. doi:10.1002/bdr2.2301.
2. de Graaf G, Buckley F, Skotko BG. Estimation of the number of people with Down syndrome in the United States. *Genet Med*. 2017;19(4):439-447. doi:10.1038/gim.2016.127.
3. Gardiner K, Herault Y, Lott IT, Antonarakis SE, Reeves RH, Dierssen M. Down syndrome: from understanding the neurobiology to therapy. *J Neurosci*. 2010;30(45):14943-14945. doi:10.1523/JNEUROSCI.3728-10.2010.
4. Walpert M, Zaman S, Holland A. A Systematic Review of Unexplained Early Regression in Adolescents and Adults with Down Syndrome. *Brain Sci*. 2021;11(9):1197. Published 2021 Sep 10. doi:10.3390/brainsci11091197.
5. Rubenstein E, Tewolde S, Michals A, et al. Alzheimer Dementia Among Individuals With Down Syndrome. *JAMA Netw Open*. 2024;7(9):e2435018. Published 2024 Sep 3. doi:10.1001/jamanetworkopen.2024.35018.
6. Saini F, Dell'Acqua F, Strydom A. Structural Connectivity in Down Syndrome and Alzheimer's Disease. *Front Neurosci*. 2022;16:908413. Published 2022 Jul 22. doi:10.3389/fnins.2022.908413.
7. Powell D, Caban-Holt A, Jicha G, et al. Frontal white matter integrity in adults with Down syndrome with and without dementia. *Neurobiol Aging*. 2014;35(7):1562-1569. doi:10.1016/j.neurobiolaging.2014.01.137.
8. Fenoll R, Pujol J, Esteba-Castillo S, et al. Anomalous White Matter Structure and the Effect of Age in Down Syndrome Patients. *J Alzheimers Dis*. 2017;57(1):61-70. doi:10.3233/JAD-161112.
9. Grzadzinski R, Mata K, Bhatt AS, et al. Brain volumes, cognitive, and adaptive skills in school-age children with Down syndrome. J Neurodev Disord. 2024;16(1):70. Published 2024 Dec 19. doi:10.1186/s11689-024-09581-6.
10. Knickmeyer RC, Gouttard S, Kang C, et al. A structural MRI study of human brain development from birth to 2 years. *J Neurosci*. 2008;28(47):12176-12182. doi:10.1523/JNEUROSCI.3479-08.2008.
11. McCann B, Levman J, Baumer N, et al. Structural magnetic resonance imaging demonstrates volumetric brain abnormalities in down syndrome: Newborns to young adults. *Neuroimage Clin*. 2021;32:102815. doi:10.1016/j.nicl.2021.102815.

12. Fukami-Gartner A, Baburamani AA, Dimitrova R, et al. Comprehensive volumetric phenotyping of the neonatal brain in Down syndrome. *Cereb Cortex*. 2023;33(14):8921-8941. doi:10.1093/cercor/bhad171.
13. Grotheer M, Rosenke M, Wu H, et al. White matter myelination during early infancy is linked to spatial gradients and myelin content at birth. *Nat Commun*. 2022;13(1):997. Published 2022 Feb 22. doi:10.1038/s41467-022-28326-4.
14. Kostović I, Sedmak G, Judaš M. Neural histology and neurogenesis of the human fetal and infant brain. *Neuroimage*. 2019;188:743-773. doi:10.1016/j.neuroimage.2018.12.043.
15. Gao W, Alcauter S, Smith JK, Gilmore JH, Lin W. Development of human brain cortical network architecture during infancy. *Brain Struct Funct*. 2015;220(2):1173-1186. doi:10.1007/s00429-014-0710-3.
16. Hamner T, Udhnani MD, Osipowicz KZ, Lee NR. Pediatric Brain Development in Down Syndrome: A Field in Its Infancy. *J Int Neuropsychol Soc*. 2018;24(9):966-976. doi:10.1017/S1355617718000206.
17. Pierpaoli C, Basser PJ. Toward a quantitative assessment of diffusion anisotropy [published correction appears in Magn Reson Med 1997 Jun;37(6):972]. *Magn Reson Med*. 1996;36(6):893-906. doi:10.1002/mrm.1910360612.
18. Jones DK, Cercignani M. Twenty-five pitfalls in the analysis of diffusion MRI data. *NMR Biomed*. 2010;23(7):803-820. doi:10.1002/nbm.1543.
19. Baburamani AA, Patkee PA, Arichi T, Rutherford MA. New approaches to studying early brain development in Down syndrome. *Dev Med Child Neurol*. 2019;61(8):867-879. doi:10.1111/dmcn.14260.
20. Guo F, Tax CMW, De Luca A, Viergever MA, Heemskerk A, Leemans A. Fiber orientation distribution from diffusion MRI: Effects of inaccurate response function calibration. *J Neuroimaging*. 2021;31(6):1082-1098. doi:10.1111/jon.12901.
21. Garic D, Al-Ali KW, Nasir A, et al. White Matter Microstructure in School-Age Children with Down Syndrome. *Dev Cogn Neurosci*. In press.
22. Romano A, Moraschi M, Cornia R, et al. White matter involvement in young non-demented Down's syndrome subjects: a tract-based spatial statistic analysis. Neuroradiology. 2018;60(12):1335-1341. doi:10.1007/s00234-018-2102-5.

23. Gunbey HP, Bilgici MC, Aslan K, et al. Structural brain alterations of Down's syndrome in early childhood evaluation by DTI and volumetric analyses. *Eur Radiol*. 2017;27(7):3013-3021. doi:10.1007/s00330-016-4626-6.

24. Verde AR, Budin F, Berger JB, et al. UNC-Utah NA-MIC framework for DTI fiber tract analysis. *Front Neuroinform*. 2014;7:51. Published 2014 Jan 9. doi:10.3389/fninf.2013.00051.

25. Prieto JC, Yang JY, Budin F, Styner M. Autotract: Automatic cleaning and tracking of fibers. *Proc SPIE Int Soc Opt Eng*. 2016;9784:978408. doi:10.1117/12.2217293.

26. Rouine J, Callaghan CK, O'Mara SM. Opioid modulation of depression: A focus on imaging studies. *Prog Brain Res*. 2018;239:229-252. doi:10.1016/bs.pbr.2018.09.007.

27. Winklewski PJ, Sabisz A, Naumczyk P, Jodzio K, Szurowska E, Szarmach A. Understanding the Physiopathology Behind Axial and Radial Diffusivity Changes-What Do We Know?. *Front Neurol*. 2018;9:92. Published 2018 Feb 27. doi:10.3389/fneur.2018.00092.

28. Aung WY, Mar S, Benzinger TL. Diffusion tensor MRI as a biomarker in axonal and myelin damage. *Imaging Med*. 2013;5(5):427-440. doi:10.2217/iim.13.49.

29. Budde MD, Xie M, Cross AH, Song SK. Axial diffusivity is the primary correlate of axonal injury in the experimental autoimmune encephalomyelitis spinal cord: a quantitative pixelwise analysis. *J Neurosci*. 2009;29(9):2805-2813. doi:10.1523/JNEUROSCI.4605-08.2009.

30. Nguyen L, Murphy K, Andrews G. Cognitive and neural plasticity in old age: A systematic review of evidence from executive functions cognitive training. *Ageing Res Rev*. 2019;53:100912. doi:10.1016/j.arr.2019.100912.

31. Rosas HD, Hsu E, Mercaldo ND, et al. Alzheimer-related altered white matter microstructural integrity in Down syndrome: A model for sporadic AD?. *Alzheimers Dement (Amst)*. 2020;12(1):e12040. Published 2020 Nov 7. doi:10.1002/dad2.12040.

32. Keller TA, Just MA. Reduced fractional anisotropy and increased radial diffusivity in high-functioning autism: A large-sample whole-brain diffusion tensor imaging study. *Neuroimage*. 2009;47(suppl 1):S68. doi:10.1016/S1053-8119(09)70386-6.

33. Song SK, Sun SW, Ramsbottom MJ, Chang C, Russell J, Cross AH. Dysmyelination revealed through MRI as increased radial (but unchanged axial) diffusion of water. *Neuroimage*. 2002;17(3):1429-1436. doi:10.1006/nimg.2002.1267.

34. Narr KL, Hageman N, Woods RP, et al. Mean diffusivity: a biomarker for CSF-related disease and genetic liability effects in schizophrenia. *Psychiatry Res*. 2009;171(1):20-32. doi:10.1016/j.pscychresns.2008.03.008.

35. Fleming V, Piro-Gambetti B, Bazydlo A, et al. Sleep and White Matter in Adults with Down Syndrome. *Brain Sci*. 2021;11(10):1322. Published 2021 Oct 5. doi:10.3390/brainsci11101322.

36. Kraguljac NV, Guerreri M, Strickland MJ, Zhang H. Neurite Orientation Dispersion and Density Imaging in Psychiatric Disorders: A Systematic Literature Review and a Technical Note. *Biol Psychiatry Glob Open Sci*. 2022;3(1):10-21. Published 2022 Jan 21. doi:10.1016/j.bpsgos.2021.12.012.

37. Andica C, Kamagata K, Kirino E, et al. Neurite orientation dispersion and density imaging reveals white matter microstructural alterations in adults with autism. *Mol Autism*. 2021;12(1):48. Published 2021 Jun 30. doi:10.1186/s13229-021-00456-4.

38. Arai T, Kamagata K, Uchida W, et al. Reduced neurite density index in the prefrontal cortex of adults with autism assessed using neurite orientation dispersion and density imaging. *Front Neurol*. 2023;14:1110883. Published 2023 Aug 11. doi:10.3389/fneur.2023.1110883.

39. Matsuoka K, Makinodan M, Kitamura S, et al. Increased Dendritic Orientation Dispersion in the Left Occipital Gyrus is Associated with Atypical Visual Processing in Adults with Autism Spectrum Disorder. *Cereb Cortex*. 2020;30(11):5617-5625. doi:10.1093/cercor/bhaa121.

40. Zhang H, Schneider T, Wheeler-Kingshott CA, Alexander DC. NODDI: practical in vivo neurite orientation dispersion and density imaging of the human brain. *Neuroimage*. 2012;61(4):1000-1016. doi:10.1016/j.neuroimage.2012.03.072.

41. Chang YS, Owen JP, Pojman NJ, et al. White Matter Changes of Neurite Density and Fiber Orientation Dispersion during Human Brain Maturation. *PLoS One*. 2015;10(6):e0123656. Published 2015 Jun 26. doi:10.1371/journal.pone.0123656.

42. Pasternak O, Sochen N, Gur Y, Intrator N, Assaf Y. Free water elimination and mapping from diffusion MRI. *Magn Reson Med*. 2009;62(3):717-730. doi:10.1002/mrm.22055.

43. Nakaya M, Sato N, Matsuda H, et al. Free water derived by multi-shell diffusion MRI reflects tau/neuroinflammatory pathology in Alzheimer's disease. *Alzheimers Dement (N Y)*. 2022;8(1):e12356. Published 2022 Oct 25. doi:10.1002/trc2.12356.

44. Takeshige-Amano H, Hatano T, Kamagata K, et al. Free-water diffusion magnetic resonance imaging under selegiline treatment in Parkinson's disease. *J Neurol Sci*. 2024;457:122883. doi:10.1016/j.jns.2024.122883.

45. Zhu H, Kong L, Li R, et al. FADTTS: functional analysis of diffusion tensor tract statistics. *Neuroimage*. 2011;56(3):1412-1425. doi:10.1016/j.neuroimage.2011.01.075.

46. Noel J, Prieto JC, Styner M. FADTTSter: Accelerating Hypothesis Testing With Functional Analysis of Diffusion Tensor Tract Statistics. *Proc SPIE Int Soc Opt Eng*. 2017;10137:1013727. doi:10.1117/12.2254711.

47. Deoni SC, Mercure E, Blasi A, et al. Mapping infant brain myelination with magnetic resonance imaging. *J Neurosci*. 2011;31(2):784-791. doi:10.1523/JNEUROSCI.2106-10.2011.

48. Brody BA, Kinney HC, Kloman AS, Gilles FH. Sequence of central nervous system myelination in human infancy. I. An autopsy study of myelination. *J Neuropathol Exp Neurol*. 1987;46(3):283-301. doi:10.1097/00005072-198705000-00005.

49. Deoni S, Dean D 3rd, Joelson S, O'Regan J, Schneider N. Early nutrition influences developmental myelination and cognition in infants and young children. *Neuroimage*. 2018;178:649-659. doi:10.1016/j.neuroimage.2017.12.056.

50. Suzuki K. Neuropathology of developmental abnormalities. *Brain Dev*. 2007;29(3):129-141. doi:10.1016/j.braindev.2006.08.006.

51. Nestor PG, Kubicki M, Gurrera RJ, et al. Neuropsychological correlates of diffusion tensor imaging in schizophrenia. *Neuropsychology*. 2004;18(4):629-637. doi:10.1037/0894-4105.18.4.629.

52. Kubicki M, Niznikiewicz M, Connor E, et al. Relationship Between White Matter Integrity, Attention, and Memory in Schizophrenia: A Diffusion Tensor Imaging Study. *Brain Imaging Behav*. 2009;3(2):191-201. doi:10.1007/s11682-009-9061-8.

53. Posner MI, Rothbart MK, Sheese BE, Tang Y. The anterior cingulate gyrus and the mechanism of self-regulation. *Cogn Affect Behav Neurosci*. 2007;7(4):391-395. doi:10.3758/cabn.7.4.391.

54. Kunz N, Zhang H, Vasung L, et al. Assessing white matter microstructure of the newborn with multi-shell diffusion MRI and biophysical compartment models. *Neuroimage*. 2014;96:288-299. doi:10.1016/j.neuroimage.2014.03.057.

55. Timmers I, Roebroeck A, Bastiani M, Jansma B, Rubio-Gozalbo E, Zhang H. Assessing Microstructural Substrates of White Matter Abnormalities: A Comparative Study Using DTI and NODDI. *PLoS One*. 2016;11(12):e0167884. Published 2016 Dec 21. doi:10.1371/journal.pone.0167884.

56. Radetz A, Mladenova K, Ciolac D, et al. Linking Microstructural Integrity and Motor Cortex Excitability in Multiple Sclerosis. Front Immunol. 2021;12:748357. Published 2021 Oct 12. doi:10.3389/fimmu.2021.748357.

57. Timmers I, Zhang H, Bastiani M, Jansma BM, Roebroeck A, Rubio-Gozalbo ME. White matter microstructure pathology in classic galactosemia revealed by neurite orientation dispersion and density imaging. J Inherit Metab Dis. 2015;38(2):295-304. doi:10.1007/s10545-014-9780-x.

58. Ji F, Pasternak O, Liu S, et al. Distinct white matter microstructural abnormalities and extracellular water increases relate to cognitive impairment in Alzheimer's disease with and without cerebrovascular disease. *Alzheimers Res Ther*. 2017;9(1):63. Published 2017 Aug 17. doi:10.1186/s13195-017-0292-4.

59. Dumont M, Roy M, Jodoin PM, et al. Free Water in White Matter Differentiates MCI and AD From Control Subjects. *Front Aging Neurosci*. 2019;11:270. Published 2019 Oct 2. doi:10.3389/fnagi.2019.00270.

60. Bazydlo A, Zammit M, Wu M, et al. White matter microstructure associations with episodic memory in adults with Down syndrome: a tract-based spatial statistics study. *J Neurodev Disord*. 2021;13(1):17. Published 2021 Apr 20. doi:10.1186/s11689-021-09366-1.

61. Salehi A, Ashford JW, Mufson EJ. The Link between Alzheimer's Disease and Down Syndrome. A Historical Perspective. *Curr Alzheimer Res*. 2016;13(1):2-6. doi:10.2174/1567205012999151021102914.

62. Ford A, Kovacs-Balint ZA, Wang A, et al. Functional maturation in visual pathways predicts attention to the eyes in infant rhesus macaques: Effects of social status [published correction appears in Dev Cogn Neurosci. 2024 Jun;67:101364. doi: 10.1016/j.dcn.2024.101364]. *Dev Cogn Neurosci*. 2023;60:101213. doi:10.1016/j.dcn.2023.101213.

63. Jones W, Klin A. Attention to eyes is present but in decline in 2-6-month-old infants later diagnosed with autism. *Nature*. 2013;504(7480):427-431. doi:10.1038/nature12715.

64. Woodhouse JM, Pakeman VH, Saunders KJ, et al. Visual acuity and accommodation in infants and young children with Down's syndrome. *J Intellect Disabil Res*. 1996;40 (Pt 1):49-55. doi:10.1111/j.1365-2788.1996.tb00602.x.

65. McDonald M, Ankrum C, Preston K, Sebris SL, Dobson V. Monocular and binocular acuity estimation in 18- to 36-month-olds: acuity card results. *Am J Optom Physiol Opt*. 1986;63(3):181-186. doi:10.1097/00006324-198603000-00003.

66. Leat SJ, Yadav NK, Irving EL. Development of Visual Acuity and Contrast Sensitivity in Children. *Journal of Optometry*. 2009;2(1):19-26. doi:10.3921/joptom.2009.19.

67. Shirazi Y, Oghabian MA, Batouli SAH. Along-tract analysis of the white matter is more informative about brain ageing, compared to whole-tract analysis. *Clin Neurol Neurosurg*. 2021;211:107048. doi:10.1016/j.clineuro.2021.107048.

68. Rieck JR, Rodrigue KM, Park DC, Kennedy KM. White Matter Microstructure Predicts Focal and Broad Functional Brain Dedifferentiation in Normal Aging. J Co*gn Neurosci*. 2020;32(8):1536-1549. doi:10.1162/jocn_a_01562.

69. Hendrix JA, Amon A, Abbeduto L, et al. Opportunities, barriers, and recommendations in down syndrome research. *Transl Sci Rare Dis*. 2021;5(3-4):99-129. doi:10.3233/trd-200090.

70. Swanson MR, Hazlett HC. White matter as a monitoring biomarker for neurodevelopmental disorder intervention studies. *J Neurodev Disord*. 2019;11(1):33. Published 2019 Dec 16. doi:10.1186/s11689-019-9295-8.

71. Carpenter KLH, Major S, Tallman C, et al. White Matter Tract Changes Associated with Clinical Improvement in an Open-Label Trial Assessing Autologous Umbilical Cord Blood for Treatment of Young Children with Autism. *Stem Cells Transl Med*. 2019;8(2):138-147. doi:10.1002/sctm.18-0251.

72. Li Z, Mei Y, Wang W, et al. White matter and cortical gray matter microstructural abnormalities in new daily persistent headache: a NODDI study. *J Headache Pain*. 2024;25(1):110. Published 2024 Jul 8. doi:10.1186/s10194-024-01815-1.

73. Collorone S, Cawley N, Grussu F, et al. Reduced neurite density in the brain and cervical spinal cord in relapsing-remitting multiple sclerosis: A NODDI study. *Mult Scler*. 2020;26(13):1647-1657. doi:10.1177/1352458519885107.

74. Friedrich P, Fraenz C, Schlüter C, et al. The Relationship Between Axon Density, Myelination, and Fractional Anisotropy in the Human Corpus Callosum. *Cereb Cortex*. 2020;30(4):2042-2056. doi:10.1093/cercor/bhz221.

75. Beaulieu C. CHAPTER 6 - The Biological Basis of Diffusion Anisotropy. In: Johansen-Berg H, Behrens TEJ, eds. *Diffusion MRI.* Academic Press; 2009:105-126. doi:10.1016/B978-0-12-374709-9.00006-7.

Figure Legends

Figure 1. Fiber tractography of the examined tracts. Abbreviations: IFOF, inferior fronto-occipital fasciculus; ILF, inferior longitudinal fasciculus; SLF, superior longitudinal fasciculus; CC, corpus callosum.

Figure 2. Violin and box plots of the significant diffusion metrics in the bilateral CST and IFOF. Abbreviations: IFOF, inferior fronto-occipital fasciculus; CST, corticospinal tract. FA, fractional anisotropy; AD, axial diffusivity; RD, radial diffusivity; NDI, neurite density index; ODI, orientation dispersion index.

Tables

Metric	*Definition of Measurement*	*Interpretation in Infants with Down syndrome*
DTI Metrics		
Fractional Anisotropy (FA)	A scalar value between 0 and 1 that quantifies the degree of anisotropy of water diffusion; 0 indicates isotropic diffusion, and 1 indicates fully anisotropic diffusion.[26]	Decreased FA values suggest a delay/disruption in the structural integrity of white matter.[6-8,23]
Axial Diffusivity (AD)	The magnitude of water diffusion parallel to the tract.[27]	Decreased AD suggests delayed/disrupted axonal organization and elongation.[28-30]
Radial Diffusivity (RD)	The magnitude of water diffusion perpendicular to the tract.[27]	Increased RD suggests delayed/disrupted myelination.[27,31-33]
Mean Diffusivity (MD)	The average amount of diffusion occurring within a single voxel.[23]	Increased MD suggests delayed/disrupted tissue organization.[6,34,35]
NODDI Metrics		
Neurite Density Index (NDI)	Reflects the fraction of tissue volume occupied by neurites (axons and dendrites).[36]	Decreased NDI suggests a delayed/disruption in neurite density.[37,38]
Orientation Dispersion Index (ODI)	The variability in neurite orientation, ranging from 0 (perfectly aligned) to 1 (randomly in all directions).[36]	Increased ODI suggests greater dispersion and fanning of neurites.[39-41]
Free Water Fraction (FWF)	The fraction of diffusion signals explained by isotopically unrestricted water, estimated using a bi-tensor model.[42]	Increased FWF suggests neuroinflammation.[43,44]

Table 1. Definitions of the DTI and NODDI parameters and their interpretation in infants with Down syndrome.

	Down syndrome (DS)	*Controls*	*Group Comparison*
N	49	37	
Sex, n (%)	Female: 28 (57.14) Male: 21 (42.86)	Female: 18 (48.65) Male: 19 (51.35)	X^2=0.611, *p*-value=0.4343
Age-at-assessment in days, Mean (SD)	207.31 (25.10)	199.62 (19.09)	t-test, *p*-value=0.1242
Gestational Age in days, Mean (SD)	n=39, 266.63 (9.46)	n=33, 272.09 (9.05)	t-test, *p*-value=0.0152*
Scan-motion quantification, Mean (SD)	10.20 (10.34)	8.92 (12.27)	t-test, *p*-value=0.6
Maternal Age at birth in years, Mean (SD)	n=38, 36.84 (4.54)	n=36, 34.16 (3.02)	t-test, *p*-value=0.004**
Paternal Age at birth in years, (Mean) (SD)	n=37, 37.71 (6.44)	n=36, 36.03 (4.96)	t-test, *p*-value=0.2171
Maternal Education, Mean (SD)	4.24 (1.30)	4.6 (1.16)	t-test, *p*-value=0.2156
1. Some high school	0 (0)	0 (0)	
2. High school graduate	3 (6.12)	0 (0)	
3. Some college	8 (16.33)	6 (16.22)	
4. College graduate	15 (30.61)	15 (40.54)	
5. Some grad school	1 (2.04)	1 (2.7)	
6. Graduate degree	11 (22.45)	13 (35.14)	
NA. Not available	11 (22.45)	2 (5.41)	
Paternal Education, Mean (SD)	4.027 (1.4237)	4.4722 (1.5021)	t-test, *p*-value=0.1978
1. Some high school	0 (0)	0 (0)	
2. High school graduate	7 (14.29)	4 (10.81)	
3. Some college	5 (10.2)	7 (18.92)	
4. College graduate	15 (30.61)	9 (24.32)	
5. Some grad school	0 (0)	0 (0)	
6. Graduate degree	10 (20.41)	16 (42.24)	
NA. Not available	12 (24.49)	1 (2.7)	
Household Income, Mean (SD)	5.8 (1.86)	6.08 (1.36)	t-test, *p*-value=0.4653
1. less than 25K	2 (4.08)	0 (0)	
2. 25K-35K	0 (0)	0 (0)	
3. 35K-50K	1 (2.04)	1 (2.70)	
4. 50K-75K	6 (12.25)	4 (10.81)	
5. 75K-100K	2 (4.08)	6 (16.22)	
6. 100K-150K	11 (22.45)	12 (32.43)	
7. 150K-200K	6 (12.25)	6 (16.22)	
8. over-200K	7 (14.29)	7 (18.92)	
NA. Not available	14 (28.57)	1 (2.70)	

Table 2. Participant demographics by group. (***p*-value is <0.0001, **p*-value is 0.01 - 0.001, *p*-value is 0.05 - 0.01).

Tract	*Parameter*	*Down syndrome (DS)*			*Controls*			*Beta value*	*Lower 95%*	*Upper 95%*	*p-value*	*Corrected p-value*	*Cohen's d*
		Mean	SD	N	Mean	SD	N						
Corpus Callosum Parietal	AD	0.001529	$3.68x10^{-5}$	47	0.001506	$3.53x10^{-5}$	35	$-1.32x10^{-5}$	$-2.13x10^{-5}$	$-5.05x10^{-6}$	0.0018**	0.009**	0.63**
	FA	0.474409	$1.93x10^{-2}$	47	0.47064	$2.56x10^{-2}$	35	$-9.36x10^{-4}$	$-5.61x10^{-3}$	$3.74x10^{-3}$	0.69	1	0.17
	NDI	0.309436	$1.95x10^{-2}$	47	0.321489	$2.27x10^{-2}$	35	$8.07x10^{-3}$	$4.06x10^{-3}$	$1.21x10^{-2}$	0.0001***	0.0005***	-0.58**
	ODI	0.095306	$8.04x10^{-3}$	47	0.098787	$9.27x10^{-3}$	35	$1.76x10^{-3}$	$-1.7x10^{-4}$	$3.7x10^{-3}$	0.073	0.37	-0.41
	RD	0.00068	$3.13x10^{-5}$	47	0.000677	$3.83x10^{-5}$	35	$-4.13x10^{-6}$	$-1.13x10^{-5}$	$3x10^{-6}$	0.25	1	0.11
Corpus Callosum Tapetum	AD	0.002154	$1.2x10^{-4}$	46	0.002089	$1.35x10^{-4}$	37	$-3.3x10^{-5}$	$-6.2x10^{-5}$	$-3.9x10^{-6}$	0.027*	0.13	0.52
	FA	0.361024	$2.42x10^{-2}$	46	0.363352	$1.65x10^{-2}$	37	$1.28x10^{-3}$	$-3.52x10^{-3}$	$6.08x10^{-3}$	0.6	1	-0.11
	NDI	0.362944	$3.6x10^{-2}$	46	0.37538	$3.14x10^{-2}$	37	$6.96x10^{-3}$	$-7.69x10^{-4}$	$1.47x10^{-2}$	0.077	0.38	-0.37
	ODI	0.190367	$3.7x10^{-2}$	46	0.183322	$3.37x10^{-2}$	37	$-2.48x10^{-3}$	$-1.05x10^{-2}$	$5.53x10^{-3}$	0.54	1	0.20
	RD	0.001231	$1.08x10^{-4}$	46	0.001194	$1x10^{-4}$	37	$-1.86x10^{-5}$	$-4.24x10^{-5}$	$5.19x10^{-6}$	0.12	0.62	0.36
CorticoSpinal Left	AD	0.001394	$4.06x10^{-5}$	49	0.00136	$4.01x10^{-5}$	37	$-1.88x10^{-5}$	$-2.76x10^{-5}$	$-1x10^{-5}$	0.00001***	0.00005***	0.84***
	FA	0.506108	$1.53x10^{-2}$	49	0.50464	$1.89x10^{-2}$	37	$-3.47x10^{-4}$	$-4.09x10^{-3}$	$3.4x10^{-3}$	0.85	1	0.09
	NDI	0.469285	$1.58x10^{-2}$	49	0.47404	$1.96x10^{-2}$	37	$2.43x10^{-3}$	$-1.46x10^{-3}$	$6.32x10^{-3}$	0.22	1	-0.27
	ODI	0.095498	$1.08x10^{-2}$	49	0.101219	$1x10^{-2}$	37	$2.81x10^{-3}$	$4.84x10^{-4}$	$5.14x10^{-3}$	0.019*	0.093	-0.55
	RD	0.000584	$2.93x10^{-5}$	49	0.000567	$3.41x10^{-5}$	37	$-9.64x10^{-6}$	$-1.65x10^{-5}$	$-2.78x10^{-6}$	0.0065**	0.033*	0.53**
CorticoSpinal Right	AD	0.001383	$4.53x10^{-5}$	48	0.001358	$4.70x10^{-5}$	37	$-1.41x10^{-5}$	$-2.43x10^{-5}$	$-4x10^{-6}$	0.0069**	0.035*	0.54**
	FA	0.507638	$1.35x10^{-2}$	48	0.510519	$1.90x10^{-2}$	37	$1.63x10^{-3}$	$-1.95x10^{-3}$	$5.21x10^{-3}$	0.37	1	-0.18
	NDI	0.467721	$1.64x10^{-2}$	48	0.469944	$2.16x10^{-2}$	37	$1.28x10^{-3}$	$-2.94x10^{-3}$	$5.5x10^{-3}$	0.55	1	-0.12
	ODI	0.095056	$8.91x10^{-3}$	48	0.096008	$7.70x10^{-3}$	37	$5.99x10^{-4}$	$-1.27x10^{-3}$	$2.46x10^{-3}$	0.52	1	-0.11
	RD	0.000576	$2.75x10^{-5}$	48	0.000556	$3.58x10^{-5}$	37	$-1.08x10^{-5}$	$-1.77x10^{-5}$	$-3.87x10^{-6}$	0.0026**	0.013*	0.63**
Inferior Fronto-Occipital Fasciculus Left	AD	0.0014	$2.65x10^{-5}$	48	0.001416	$4.57x10^{-5}$	35	$6.94x10^{-6}$	$-8.34x10^{-7}$	$1.47x10^{-5}$	0.079	0.4	-0.44
	FA	0.395741	$1.67x10^{-2}$	48	0.417533	$1.47x10^{-2}$	35	$1.16x10^{-2}$	$7.97x10^{-3}$	$1.51x10^{-2}$	0.00001***	0.00005***	-1.37***
	NDI	0.291474	$1.35x10^{-2}$	48	0.302593	$1.93x10^{-2}$	35	$6.86x10^{-3}$	$3.53x10^{-3}$	$1.02x10^{-2}$	0.0001***	0.0005***	-0.69**
	ODI	0.126647	$9.4x10^{-3}$	48	0.115319	$9.39x10^{-3}$	35	$-5.83x10^{-3}$	$-7.8x10^{-3}$	$-3.85x10^{-3}$	0.00001***	0.00005***	1.21***
	RD	0.000743	$2.5x10^{-5}$	48	0.000718	$2.77x10^{-5}$	35	$-1.38x10^{-5}$	$-1.96x10^{-5}$	$-8.09x10^{-6}$	0.00001***	0.00005***	0.94***

Inferior Fronto-Occipital Fasciculus Right	AD	0.001407	$2.7x10^{-5}$	45	0.001416	$4.60x10^{-5}$	35	$2.01x10^{-6}$	$-5.99x10^{-6}$	$1x10^{-5}$	0.62	1	-0.25
	FA	0.400235	$1.69x10^{-2}$	45	0.415485	$1.48x10^{-2}$	35	$8.66x10^{-3}$	$4.96x10^{-3}$	$1.24x10^{-2}$	0.00001***	0.00005***	-0.95***
	NDI	0.29	$1.51x10^{-2}$	45	0.301486	$1.84x10^{-2}$	35	$7.75x10^{-3}$	$4.3x10^{-3}$	$1.12x10^{-2}$	0.00001***	0.00005***	-0.69**
	ODI	0.120209	$9.47x10^{-3}$	45	0.112315	$1.06x10^{-2}$	35	$-3.94x10^{-3}$	$-6.18x10^{-3}$	$-1.71x10^{-3}$	0.0007***	0.0035**	0.79**
	RD	0.000742	$2.51x10^{-5}$	45	0.000722	$2.67x10^{-5}$	35	$-1.3x10^{-5}$	$-1.85x10^{-5}$	$-7.53x10^{-6}$	0.00001***	0.00005***	0.79**
Inferior Longitudinal Fasciculus Left	AD	0.001502	$3.31x10^{-5}$	35	0.001481	$6.48x10^{-5}$	37	$-1.28x10^{-5}$	$-2.52x10^{-5}$	$-3.33x10^{-7}$	0.044*	0.22	0.41
	FA	0.40438	$2.19x10^{-2}$	35	0.417521	$2.16x10^{-2}$	37	$6.57x10^{-3}$	$1.23x10^{-3}$	$1.19x10^{-2}$	0.017*	0.084	-0.60
	NDI	0.276527	$1.74x10^{-2}$	35	0.294301	$2.33x10^{-2}$	37	$1.03x10^{-2}$	$5.63x10^{-3}$	$1.5x10^{-2}$	0.00001***	0.00005***	-0.86***
	ODI	0.107502	$8.26x10^{-3}$	35	0.109542	$1.11x10^{-2}$	37	$1.35x10^{-3}$	$-1.04x10^{-3}$	$3.75x10^{-3}$	0.26	1	-0.21
	RD	0.000781	$3.28x10^{-5}$	35	0.000755	$3.96x10^{-5}$	37	$-1.39x10^{-5}$	$-2.26x10^{-5}$	$-5.1x10^{-6}$	0.0024**	0.012*	0.69**
Inferior Longitudinal Fasciculus Right	AD	0.001542	$5.42x10^{-5}$	37	0.001521	$6.07x10^{-5}$	37	$-1.42x10^{-5}$	$-2.71x10^{-5}$	$-1.34x10^{-6}$	0.031*	0.16	0.36
	FA	0.41299	$2.4x10^{-2}$	37	0.428126	$2.08x10^{-2}$	37	$7.12x10^{-3}$	$1.7x10^{-3}$	$1.25x10^{-2}$	0.011*	0.054	-0.67
	NDI	0.271777	$2.1x10^{-2}$	37	0.28743	$2.23x10^{-2}$	37	$9.43x10^{-3}$	$4.65x10^{-3}$	$1.42x10^{-2}$	0.0002***	0.001**	-0.72**
	ODI	0.104156	$9.87x10^{-3}$	37	0.104143	$8.91x10^{-3}$	37	$5.59x10^{-4}$	$-1.48x10^{-3}$	$2.6x10^{-3}$	0.59	1	0.00
	RD	0.000792	$3.7x10^{-5}$	37	0.000765	$3.92x10^{-5}$	37	$-1.45x10^{-5}$	$-2.35x10^{-5}$	$-5.49x10^{-6}$	0.002**	0.01*	0.7**
Superior Longitudinal Fasciculus II Left	AD	0.001336	$3.23x10^{-5}$	40	0.001332	$4.41x10^{-5}$	29	$-3.85x10^{-6}$	$-1.3x10^{-5}$	$5.31x10^{-6}$	0.4	1	0.1
	FA	0.332468	$1.71x10^{-2}$	40	0.355197	$2.01x10^{-2}$	29	$1.18x10^{-2}$	$7.36x10^{-3}$	$1.62x10^{-2}$	0.00001***	0.00005***	-1.23***
	NDI	0.273937	$1.56x10^{-2}$	40	0.289206	$2.07x10^{-2}$	29	$9.32x10^{-3}$	$5.53x10^{-3}$	$1.31x10^{-2}$	0.00001***	0.00005***	-0.85***
	ODI	0.16971	$1.43x10^{-2}$	40	0.152933	$1.47x10^{-2}$	29	$-7.98x10^{-3}$	$-1.16x10^{-2}$	$-4.32x10^{-3}$	0.00001***	0.00005***	1.16***
	RD	0.000798	$2.81x10^{-5}$	40	0.000766	$3.45x10^{-5}$	29	$-1.78x10^{-5}$	$-2.49x10^{-5}$	$-1.08x10^{-5}$	0.00001***	0.00005***	1.03***
Superior Longitudinal Fasciculus II Right	AD	0.001328	$3.23x10^{-5}$	33	0.001327	$4.37x10^{-5}$	34	$-2.64x10^{-6}$	$-1.16x10^{-5}$	$6.32x10^{-6}$	0.56	1	0.02
	FA	0.339356	$2.07x10^{-2}$	33	0.354572	$1.66x10^{-2}$	34	$8.21x10^{-3}$	$3.62x10^{-3}$	$1.28x10^{-2}$	0.0007***	0.0035**	-0.81***
	NDI	0.279004	$1.67x10^{-2}$	33	0.293487	$1.92x10^{-2}$	34	$8.78x10^{-3}$	$5.14x10^{-3}$	$1.24x10^{-2}$	0.00001***	0.00005***	-0.8***
	ODI	0.160886	$1.53x10^{-2}$	33	0.152281	$1.35x10^{-2}$	34	$-4.42x10^{-3}$	$-8.01x10^{-3}$	$-8.38x10^{-4}$	0.016*	0.082	0.6
	RD	0.000778	$3.02x10^{-5}$	33	0.000758	$3.02x10^{-5}$	34	$-1.2x10^{-5}$	$-1.86x10^{-5}$	$-5.39x10^{-6}$	0.0006***	0.003**	0.66**
	AD	0.001386	$2.94x10^{-5}$	39	0.001397	$3.54x10^{-5}$	36	$3.48x10^{-6}$	$-3.97x10^{-6}$	$1.09x10^{-5}$	0.35	1	-0.32

Uncinate Fasciculus Left	FA	0.370956	$1.65x10^{-2}$	39	0.383937	$1.38x10^{-2}$	36	$7.23x10^{-3}$	$3.62x10^{-3}$	$1.08x10^{-2}$	0.0002***	0.001**	-0.85***
	NDI	0.271155	$1.57x10^{-2}$	39	0.27973	$1.95x10^{-2}$	36	$5.81x10^{-3}$	$1.88x10^{-3}$	$9.73x10^{-3}$	0.0043**	0.022*	-0.49*
	ODI	0.147031	$1.17x10^{-2}$	39	0.138847	$1.05x10^{-2}$	36	$-3.78x10^{-3}$	$-6.36x10^{-3}$	$-1.2x10^{-3}$	0.0046**	0.023*	0.73**
	RD	0.000772	$2.52x10^{-5}$	39	0.000757	$2.56x10^{-5}$	36	$-9.21x10^{-6}$	$-1.49x10^{-5}$	$-3.52x10^{-6}$	0.0019**	0.0095**	0.56**
Uncinate Fasciculus Right	AD	0.001389	$2.92x10^{-5}$	40	0.001409	$3.76x10^{-5}$	37	$8.49x10^{-6}$	$1.01x10^{-6}$	$1.60x10^{-5}$	0.027*	0.13	-0.6
	FA	0.360311	$1.41x10^{-2}$	40	0.376878	$1.47x10^{-2}$	37	$8.78x10^{-3}$	$5.59x10^{-3}$	$1.2x10^{-2}$	0.00001***	0.00005***	-1.15***
	NDI	0.263935	$1.51x10^{-2}$	40	0.27032	$1.93x10^{-2}$	37	$4.2x10^{-3}$	$4.67x10^{-4}$	$7.94x10^{-3}$	0.028*	0.14	-0.37
	ODI	0.14925	$1.1x10^{-2}$	40	0.13898	$1.09x10^{-2}$	37	$-4.97x10^{-3}$	$-7.5x10^{-3}$	$-2.44x10^{-3}$	0.0002***	0.001**	0.94***
	RD	0.000785	$2.56x10^{-5}$	40	0.000768	$2.81x10^{-5}$	37	$-1x10^{-5}$	$-1.58x10^{-5}$	$-4.23x10^{-6}$	0.0009***	0.0045**	0.64**

Table 3. Results of univariate analyses of variance comparing DTI and NODDI parameters in the significant tracts between DS and control infants.
(****p*-value is <0.0001, ***p*-value is 0.01 - 0.001, **p*-value is 0.05 - 0.01; Cohen's d: *small effect is 0.2 – 0.5, **medium effect is 0.5 – 0.8, ***large effect is ≥ 0.8).

Figure 1

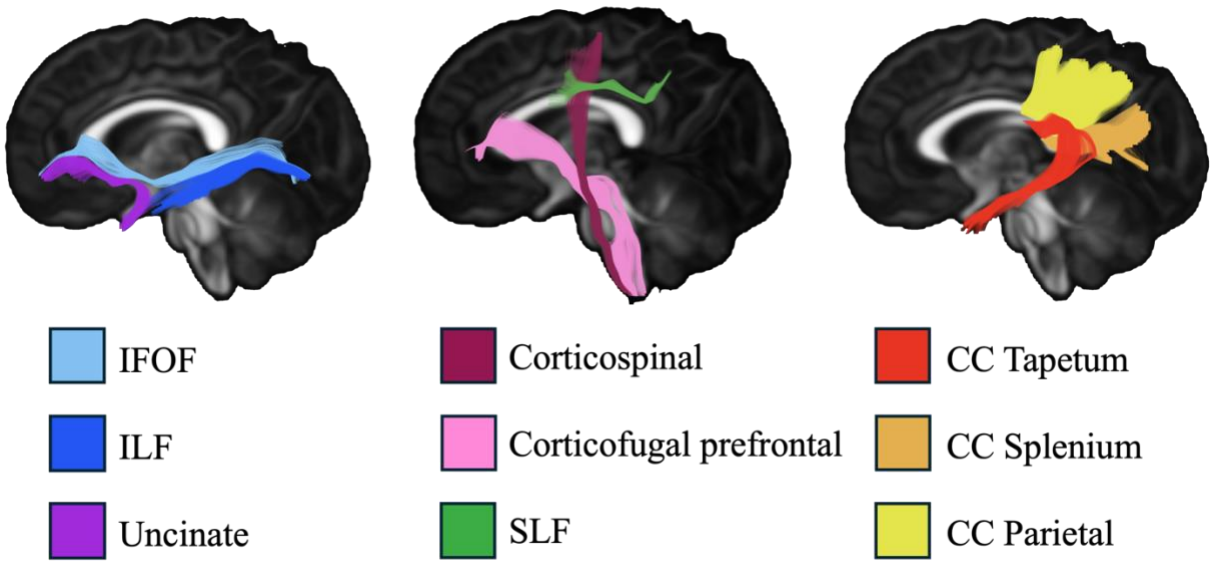

Figure 2